Shape-from-focus for real-time terahertz 3D imaging

J.-B. Perraud, J.-P. Guillet, O. Redon, F. Simoens, Patrick Mounaix

Shape from Focus for Real-Time Terahertz 3D Imaging

J-B PERRAUD[1, 2], J-P GUILLET[1], O. REDON[2], F.SIMOENS[3] AND P.MOUNAIX[1]

[1]*IMS – Bordeaux University, Bât. A31, 351 Cours de la Libération, 33400 Talence, France*
[2]*CEA Tech Nouvelle-Aquitaine, Cité de la Photonique – Bât. SIRAH Allée des lumières 33600 Pessac, France*
[3]*CEA LETI, 17 rue des Martyrs 38054 Grenoble Cedex 9, France*

*Corresponding author: Patrick Mounaix patrick.mounaix@u-bordeaux.fr

Received XX Month XXXX; revised XX Month, XXXX; accepted XX Month XXXX; posted XX Month XXXX (Doc. ID XXXXX); published XX Month XXXX

Thanks to significant advances in real-time terahertz imaging in term of resolution and image quality, the possibilities for 3D reconstruction are numerous. The Shape from Focus (SFF) algorithm is a post-processing tool used in optical microscopy to obtain the 3D object shape surface. It allows the object reconstruction even if it is positioned out of focus of the optical system. In this letter, we propose an application of this algorithm in active and real-time terahertz imaging. We notably achieve the experimental reconstruction of a 3D terahertz object.

Terahertz (THz) frequency range radiation, 0.3–10THz, has shown promises for security and biomedical imaging applications because of spectral absorption features that allow cancer differentiation [1][2] or unique absorption peaks in illicit drugs for screening purposes [3]. Real-time terahertz imaging is a growing interest and necessary for democratization of this science and transfer to industry. Microbolometer focal plane arrays (FPAs) have recently been developed specifically for the THz frequency range by several research groups. With a resolution and a signal to noise ratio comparable with raster scan technics, the full field terahertz imaging allows 3D reconstruction [4][5] in a short time of acquisition [6], revealing the inside of an optically opaque object. Among all methods to obtain a 3D reconstruction, the terahertz computed tomography (CT) is the most efficient tool. However, for 2D bended samples or samples with high aspect ratio, the terahertz CT is not adapted for 3D reconstruction.

Moreover, the focus of terahertz beams with optical elements for terahertz waves from the sample to produce a sharp image is still complicated. In optics, a specific sample plane is intrinsically defined so that samples that are not located exactly in the sample plane are out of focus. In high-resolution microscopy, the depth of field (DOF) is typically a micrometer or less. The depth of field depends on four parameters: distance (D), aperture (A), focal length (F) and radius of the circle of confusion (C). The selection of all these parameters will affect not only the depth of field (DoF) but also the available field of view (FoV).

As consequence, samples are often larger than the DOF and it is necessary to refocus the image throughout its depth to form a clear picture. In a recent approach facilitated by numerical microscope, a 'Z-stack' of images are recorded and numerically treated to reconstruct a clear image with an extended DOF.

One possible numerical approach of the image processing method called Shape from Focus (SFF) is presented in [7]. Basically, it uses the defocusing effect in the imaging system to create a surface depth map. By changing the object position along the optical axis, a stack of blurred and clear images is acquired. The measurement of the focus at each pixel of all the images is used to get the 3D depth map of the object.

In this letter, we propose to apply shape from focus post-processing algorithm to real time terahertz images in transmission mode. Then a THz sharp image can be obtained in real time without any modification of the optics.

The idea of varying the sharpness of an image to measure the distance between the object and the imaging system was proposed and studied in 1968 [8] thanks to a discrete Fourier transform. Another technique, more robust than the previous one when the images show strong differences in texture (intensity variations from one pixel to another) is described in [7] and applied to reflection optical microscopy. It consists in moving the sample along the z-axis around the focal plane and measuring a focus ψ from the sum of the second derivative of the intensity I (X, Y) along the x and y axis (Laplacian). The maximum value of ψ enables an evaluation of the position of the object along the z axis. The SFF algorithm uses the sum of the modified Laplacian (ML) operator [7] on each pixel of all the images to calculate the focus versus the optical axis. Then, a focus measure at the pixel (x, y, z) is calculated by:

$$F(x,y,z) = \sum_{X=x-N}^{x+N} \sum_{Y=y-N}^{y+N} ML(X,Y,z) \;\; if \;\; ML > T$$

N determines the window size to compute the focus measurement. T is a threshold value to remove contribution of the too-low contrasted region of the images. The sharpest pixel is given by the maximum value $F_m(x,y,d) = \max(F(x,y,z))$ at the position $z = d$. A more accurate method to find the best focus consists in interpolating F along the z axis, considering a Gaussian distribution, also described in [7] :

$$F(x,y,z) = F_p(x,y)e^{-\frac{1}{2}\left(\frac{z-\bar{d}(x,y)}{\sigma}\right)^2}$$

With F_p, the new maximum focusing value, and $\bar{d}$, the new best focusing z position. σ is the depth of field of the terahertz imaging system, considered constant all over the image area.

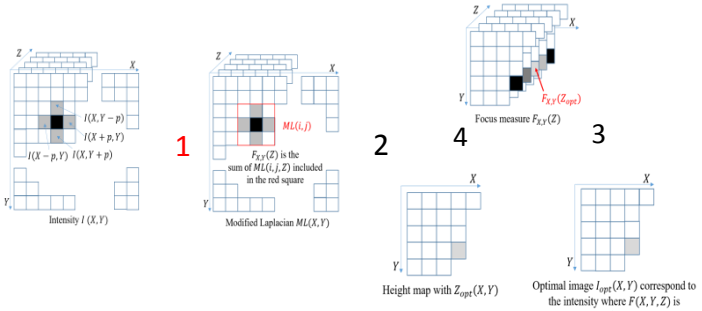

Fig1. : description of the different calculation steps to extract the maximum of F and the height map

Fig1. describes the different calculation steps to extract the maximum of F and the height map from a set of raw images acquired in real time with the experimental setup. A description of different mathematical operators for shape-from-focus technique could be found in [9]

For the experiment, a 2.5 THz quantum cascade laser cooled in closed circuit at 44 K is used. The source at 2.5 THz is the commercial compact laser TeraCascade 1000 (TC 1000) provided by the company Lytid with a maximum power of 3 mW. The laser cooling is carried out using a cryogenic Stirling pump previously put under a primary vacuum. The QCL laser is powered by a high frequency (> 10 kHz) modulated voltage to limit their heating and with a variable duty cycle (RC) to control the output power. An over-modulation of the voltage by a function generator can be used to synchronize the detection. a high-resistivity silicon hemispherical lens is attached At the output of the chip to ensure better impedance matching between the QCL chip and the vacuum : the emission profile in free space THz beam is thus better controlled. The QCL laser requires a secondary vacuum for cryogenic cooling, a high resistivity silicon window associated with a parylene antireflection treatment makes it possible to ensure tightness and excellent transparency to terahertz radiation. It is interesting to note that at 2.5 THz, almost the entire object plane of 64 * 48 mm2 is uniformly illuminated with an SNR of more than 30 dB on each pixel. A ¼ magnification objective (field of view : 64*48 mm^2) was designed its depth of field is estimated~ 6 mm (Rayleigh distance = 3 mm).To perform the Z-scanning process, a linear stage moving the sample along z axis is implemented with a continuous displacement of 1.25 mm/s . The object is moving along z axis while the camera acquisition frame rate is 25 fps: the step size between two images is equal to 50 µm.

To test the validity of the numerical procedure, we firstly image a dried oak leaf (FIG. 2 (a)). To ensure that all parts of the sheet are at least once in the focal plane, the focal plane is displaced 12.5 mm along the optical axis at a constant speed of 1, 25mm / s.

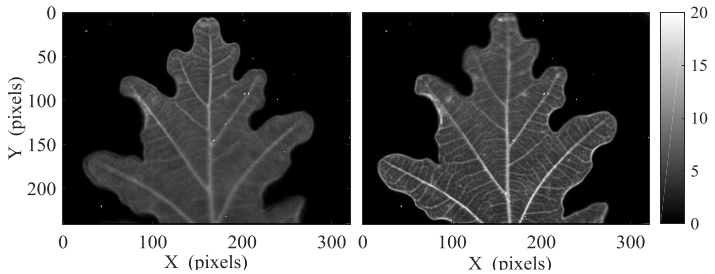

Figure 2 (a) Photo of a dried oak leaf (b) Selection among 250 images of absorbance (0-20 dB) at 2.5 THz of the oak leaf.

From a series of 250 images obtained in 10 seconds, we present two of them. Sharpness variations can be noted between the two images of Fig.2b but also between parts of the same image. You can access the raw data video of the acquisition.

We can observe that the nervures of the leaf are clearly resolved, nonetheless they appeared blurred because of their position out of the DOF.

For each image, the modified Laplacian is calculated using the 4 closest neighbours of each pixel, the sum is performed on a centered 11*11 pixels (N=5) square around each pixel and the threshold value of the ML is 3 dB.

In Fig.3 the focus measurement on three pixels reveals a maximum value strongly dependent on the relative position along the z axis. Z is the position of the first image. We find that *F(z)* may be assumed to have a Gaussian distribution with a mean value *d* and a standard deviation. It can be noted that we can easily model and extract the maximum of F for each of the pixels and that the width σ_0 of F(z) is of the same order of magnitude as the Rayleigh length, approximately 3 mm.

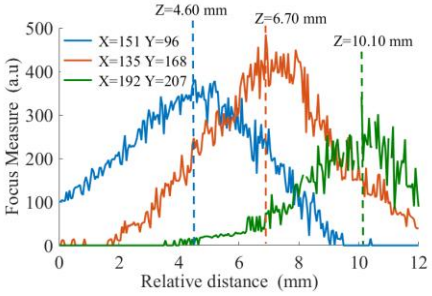

Fig.3. Focus measure of three pixels with coordinates (X, Y) of the dried oak leaf images

The interpolation is used to find the maximum value and position of focusing along the optical axis, and obtain an optimal image in Fig.4where clearly no part of the picture is blurred. Because of a dozen of dead pixels over the 76800 pixels of the array, some regions have not found the good focusing and some black square could be displayed.

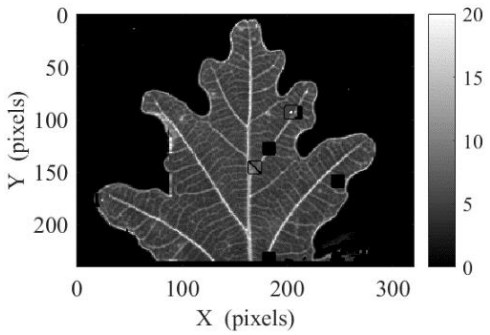

Fig. 4. Optimal absorbance gray scale image of the dried oak leaf processed by SFF algorithm

When a focus value is allocated to each pixel of all the images, these results are used to obtain the depth information. Indeed, a curve is obtained for each point of the sample and we can record the maximum of this curve to determine in which image the point is the sharpest. Once this is performed for all pixels, we associate a gray level to each point according to the sharp position to obtain the depth map given Fig.5. We present a mapping of the relief of the sheet Zmax (X, Y) given in mm, thus taking up the curved 3D shape of the oak leaf.
This depth map permits us to separate the different pixels that are not located on the same spatial plane. The knowledge of spatial location of each pixel allow us to reconstruct the shape of the object in three dimensions. Thus, with the focus measure values, we can create a merged image to retrieve a 2D image from the sequence with the best sharpness as possible as displayed in Fig3. This study shows the possibility of reconstructing objects whose radial dimension is very large in front of the transverse dimension.

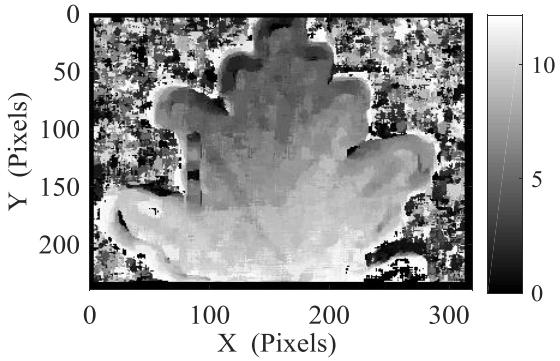

Fig.5: Depth Map of the oak leaf , the unit in mm

To go further, we tested this new approach with an object presenting good penetration properties with respect to the terahertz frequency[10]. For example, terahertz imaging has been used for the measurements of papyrus texts, including images of hidden papyri and reading through two sheets [11]. To this aim, we added a maple leaf over the oak leaf previously imaged. The gap separating the two sheets is between 10 and 20 mm. The two images in Fig.6(b) were selected from a series of 1292 images to focus on a portion of the maple leaf (left) and part of the oak leaf (right). In each of the images, however, we find an absorption induced by the oak leaf (on the left) and the maple leaf (on the right), which can affect the representation of the object. In Fig.6, the evolution of F(z) on the pixel (X = 125 and Y = 175) reveals this time two local maxima, the first corresponding to the estimated maximum maple leaf position, the second related to that of the oak leaf. The focusing measurement clearly exhibit more than one local maximum along the optical axis. The search for the maximum by using only the interpolation with these two peaks proved to be inefficient for obtaining an optimal image without filtering. We therefore applied a second-order Butterworth filter on F(z) for all the pixels with a cut-off frequency of 1 mm-1, making it possible to find the two maximums automatically after interpolation. The search for the position of the two maximum local two local maxima is carried out considering first, that there is a continuity of the surface of the leaves and that secondly. The position of the maple leaf is less than the oak one. Images of the second sample taken at two different z positions are presented in Fig.6 Despite the presence of a second leaf close to the first, the short depth of field of the lens allows imaging and identification of the hidden oak leaf behind the maple leaf.

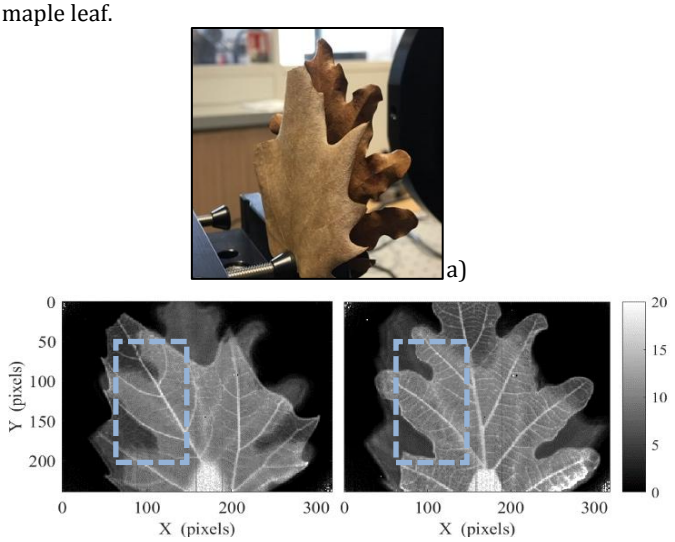

b) Fig. 6. Images of the second sample taken at two different z positions revealing the hidden oak leaf behind the maple leaf

The calculation of F for one pixel in Fig. . with the two leaves could be too noisy to directly find the two maximum values and positions. Therefore, a second order low-pass Butterworth filter along z axis at the cut-off frequency of 1 mm^{-1} is applied on F before interpolation. Then a double gaussian shape could be resolved and simulated given then the access of the individual position of end layer. In Fig. , optimal images of the selected area are pasted on the height map to reveal the 3D bended shape of the two leaves.

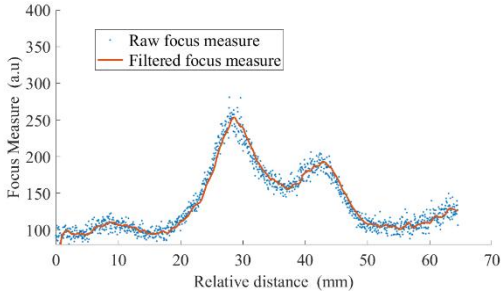

Fig. 7. Focus measure of the pixel (X=125, Y=175) revealing two peaks corresponding to the position of the two leaves

The use of this new vision systems allows us to obtain some particular characteristics of the sample. In fact, the parameters that require depth information of the sample, like some defects, the determination of sample volume, the sample surface is possible.

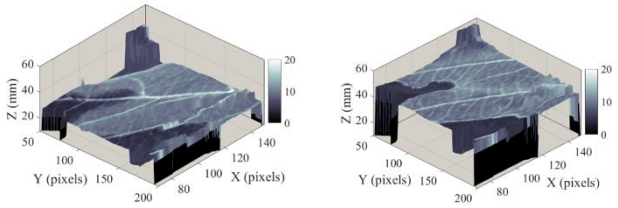

Fig. 8. A) . Focus measure of the pixel (X=125, Y=175) revealing two peaks corresponding to the position of the two leaves b) 3D reconstructed bended shape of the maple leaf using the first optimal image pasted on the first height map

A video2 allows to reconstruct in 3 dimensions the detail of each leaf and also the relative position. The influence of the absorption by the oak leaf can be observed on the optimal image of the maple leaf. However, despite the strong contrast (> 10 dB) induced by the edge of the oak leaf, the determination of the position of the maximum makes it possible to find the 3D shape of each leaf. In this reconstruction, the depth of field plays a capital role; for reasons of Gaussian overlap, the distance between the surfaces to be reconstructed must be greater than $\sigma_0 = z_R$. That criterion limits the transverse optical resolution of a 3D reconstruction obtained by the SFF algorithm. The resolution at 2.5 THz in the 3 dimensions of the reconstruction is therefore equal to Xres=0,35mm, Yres=0,35mm and Zres equal to 3mm.

As a conclusion, we demonstrated the possibility to reconstruct 3D bended shape samples using a 2.5 THz real-time imaging system. The SFF algorithm is well suited when the object is too thin to be reconstructed by terahertz computed tomography. By calculating the modified Laplacian on each pixel of the 250 partially blurred images acquired in real time, we provide a sharp image and the depth map of one sample but also on two stacked samples. Due to transparency of certain materials to terahertz wave, this approach permits volume inspection of one object or piled samples with the resolution limited by the optics, 3mm in the present case. This new terahertz reconstruction method could be applied for Non-Destructive Testing of new manufactured parts made from optically opaque materials. Future works will focus on improving the existing system and mainly on the optical part to improve the accuracy by decreasing the depth of field. An important point for any use of this acquisition method is the tradeoff between accuracy and the available field of view, because both are linked and depend on the user's needs or requirements.

Acknowledgments: Funding from Région Nouvelle Aquitaine in the 3R3D project

References

. [1] C. Am Weg, W. Von Spiegel, R. Henneberger, R. Zimmermann, T. Loeffler, and H. G. Roskos, "Fast active THz cameras with ranging capabilities," *J. Infrared, Millimeter, Terahertz Waves*, vol. 30, no. 12, pp. 1281–1296, 2009.

[2] M. R. Grootendorst *et al.*, "Use of a handheld terahertz pulsed imaging device to differentiate benign and malignant breast tissue," *Biomed. Opt. Express*, vol. 8, no. 6, p. 2932, 2017.

[3] J. B. Sleiman, B. Bousquet, N. Palka, and P. Mounaix, "Quantitative Analysis of Hexahydro-1,3,5-trinitro-1,3,5, Triazine/Pentaerythritol Tetranitrate (RDX–PETN) Mixtures by Terahertz Time Domain Spectroscopy," *Appl. Spectrosc.*, vol. 69, no. 12, pp. 1464–1471, 2015.

[4] H. Balacey, J.-B. Perraud, B. Recur, and P. Mounaix, "Processing sequence to analyse 3D THz images," in *International Conference on Infrared, Millimeter, and Terahertz Waves, IRMMW-THz*, 2014.

[5] J. P. Guillet *et al.*, "Review of terahertz tomography techniques," *J. Infrared, Millimeter, Terahertz Waves*, vol. 35, no. 4, 2014.

[6] F. Simoens *et al.*, "Towards industrial applications of terahertz real-time imaging," 2018, vol. 10531, no., p. 105310T–10531–11.

[7] S. K. Nayar and Y. Nakagawa, "Shape from Focus," *IEEE Trans. Pattern Anal. Mach. Intell.*, vol. 16, no. 8, pp. 824–831, 1994.

[8] B.K.P Horn, "Focusing.pdf," *MIT Artif. Intell. Lab.*, vol. Memo No. 1, 1968.

[9] S. Pertuz, D. Puig, and M. A. Garcia, "Analysis of focus measure operators for shape-from-focus," *Pattern Recognit.*, vol. 46, no. 5, pp. 1415–1432, 2013.

[10] J. B. J. B. Perraud *et al.*, "Terahertz imaging and tomography as efficient instruments for testing polymer additive manufacturing objects," *Appl. Opt.*, vol. 55, no. 13, pp. 3462–3467, 2016.

[11] J. Labaune, J. B. Jackson, S. Pagès-Camagna, I. N. Duling, M. Menu, and G. A. Mourou, "Papyrus imaging with terahertz time domain spectroscopy," *Appl. Phys. A Mater. Sci. Process.*, vol. 100, no. 3, pp. 607–612, 2010.

.